Astrodynamics Vol. 3, No. 1, 1–15, 2019 https://doi.org/10.1007/s42064-018-0032-y

Solar sail *H*-reversal trajectory: A review of its advances and applications

Xiangyuan Zeng[1] (✉), **Giovanni Vulpetti**[2], **and Christian Circi**[3]

1. School of Automation, Beijing Institute of Technology, Beijing 100081, China
2. International Academy of Astronautics, Paris 75116, France
3. Sapienza University of Rome, Rome 00138, Italy

ABSTRACT

The set of the orbital angular-momentum reversal, or *H*-reversal, sailcraft trajectory was born as a type of unconventional precursor interstellar mission trajectory by using high-performance solar sails. Starting from an outline of the *H*-reversal sail trajectory, this paper mainly focuses on the 2D reversal-mode solution to the general solar-photon sail motion equations. The feasible region for *H*-reversal trajectories in fixed sail attitude angles is illustrated. Some interesting applications of the *H*-reversal trajectory are presented in detail to show its advantages. As a special case, a precursor interstellar probe can be delivered with a constant sail orientation in the *H*-reversal trajectory to be compared with the direct-motion sail flyby of the Sun. Of importance are the heliocentric periodic orbits in double *H*-reversal modes, obtained via both fixed and time-varying sail attitude angles. Two more applications involving *H*-reversal trajectories are discussed in terms of asteroid deflection and transfer trajectory to rectilinear orbits. Finally, some items of the mathematics behind the 3D motion-reversal trajectories are summarized.

KEYWORDS
solar-photon sailing
sailcraft
lightness number
orbital *H*-reversal mode

Review Article
Received: 24 February 2018
Accepted: 04 April 2018

1 Introduction

As one of the ambitious goals of humankind, interstellar missions have been attracting attentions from both science communities and technical fields since the Fifties. With the successful launch of the two Voyager spacecraft and continuously refreshing the records of deep space distances over the past few decades, the knowledge of the outer solar system has been expanded remarkably by the transmitted data. At the time of this writing, Voyager 1 has arrived at 139.6 AU from the Sun (after 40 years from launch) by a cruise speed of 3.5 AU/yr with respect to the Sun (1 AU/yr = 4.74047 km/s). In 2006 another spacecraft named 'New Horizons' was launched by NASA to explore the Pluto system as well as one or more Kuiper belt objects. Such activities have undoubtedly encouraged the research interest of in-situ explorations of the heliopause and interstellar space beyond 200 AU in a life working duration (i.e., usually 35 years). For instance, NASA-JPL proposed an Interstellar Probe mission of 200 AU within 15 years [1], whereas ESA expected to take 25 years to achieve the same distance by a very preliminary deep-space sail mission concept [2].

An exciting project, started by NASA-JPL, suggested that a solar sail spacecraft can reach 200 AU in less than 20 years in the direction of the solar apex [3], just to begin with. The launch windows for these time-optimal trajectories are in June every year referred to as 'the June opportunity'. Almost in parallel, another creative study, fostered by Marshall Space Flight Center (MSFC) of NASA and led by Johnson and Leifer [4], found that there is an additional launch opportunity in October, every year [5] (referred to as 'the October opportunity'). To carry out interstellar missions with low cost and high reliability, it is of high concern to have two launch windows every year. Moreover, the 3D trajectory related to 'the October opportunity' can be segmented in few arcs implemented each with its own constant sail attitude for most of the mission (i.e., only

✉ zeng@bit.edu.cn

about 20 days entail a time-varying sail attitude that however is simple to carry into effect). All this makes the flight of an interstellar probe more reliable from the attitude control point of view [4]. In addition, some of the trajectory cruise speeds resulted higher than 20 AU/yr.

Researchers have to face with many challenges in order to realize the very advanced missions, including but not limited to trajectory design, very deep space communication, high specific power systems, and high performance thermal protection systems [6]. It is clear that chemical rocket propulsion is ruled out due to its low specific impulse. Thus, one would need non-chemical or non-rocket propulsion systems for getting spacecraft's final speeds higher than 10 AU/yr, and also for avoiding planning a high number of gravity-assist maneuvers, which would increase the flight time significantly. Propulsion systems such as the solar/nuclear electric propulsion (SEP/NEP) have been proposed and extensively investigated since the Sixties. From this point of view, interstellar precursor missions (IPMs) will not only enhance our knowledge of the solar system boundaries and notably beyond, but also promote theoretical innovations and technological advancements.

One of the innovative propulsion systems is the solar sail for which there is no fuel consumption. Solar sails are usually large and very thin membranes on which the solar radiation pressure (SRP) acts [7]. Thrust arises from the many-feature interaction between the incident electromagnetic waves and the sail surface, including its roughness. Solar-Photon Sailing (SPS) is a non-rocket type of propulsion system with its first successful flight in May 2010 (IKAROS/JAXA). However, the concept of SPS can be dated back to the 1920s with the great visions of Tsiolkovsky and Tsander. The increasing interest in the scientific research into solar sails began with a NASA/JPL project: an envisaged mission to the Halley comet for rendezvous in 1986; however, that remarkable project did not become a reality for some historical causes. From the initial concept of solar sail to the current successful flights (IKAROS/JAXA, Nanosail-D2/NASA, LightSail-A/Planetary Society), a century has passed where numerous theoretical and technological advances, related to the nanotechnology, have been taking place, and could result in notable progress of SPS in the near term. Currently, more mature propellantless systems are in progress at NASA and JAXA.

To decrease the flight time as much as possible, a technique of Solar Photonic Assist (SPA) [8] was suggested for sail-based IPMs. Even with the SPA flyby, IPM probes will require high performance solar sails. For example, Dachwald [9] investigated the Neptune flyby scenario by using a solar sail with a characteristic acceleration a_c of 0.5 mm/s^2. By three SPA flybys at 0.1 AU closest distance seen in Fig. 1(a), it still takes more than six years to arrive at the Neptune. As for a single SPA flyby, Sauer [3] obtained a set of optimized solutions where sail jettisoning at 5 AU is assumed as illustrated in Fig. 1(b). This interstellar precursor probe may achieve a cruise speed of 10.9 AU/yr by using a solar sail with characteristic acceleration of 2.4 mm/s^2. In this case, the orbital perihelion is set to be 0.3 AU, which is by far easier to be implemented compared to the case for 0.1 AU.

Sauer's results are attractive because 100 AU missions can be carried out in 10 years, the minimum reasonable time to cruising for an IPM. Note that such trajectories need time-varying sail attitudes to produce true minimum-time solutions [10]. However, due to the limitation of sail reorientation under realistic attitude constraints, some optimal attitude profiles cannot be implemented, in practice. For these interstellar missions, high performance sails are expected to have linear sizes of the order of 1 km, thus resulting in a great challenge of attitude control by methods not using nanotech materials as actuators.

In a way like logarithmic spiral trajectories, a novel approach with sail attitude angles constant in the sailcraft's heliocentric orbital frame (HOF) was proposed by Vulpetti [10] in 1992 for dealing with interstellar precursor missions. A so-controlled trajectory is referred to as the 'H-reversal trajectory' as it achieves a single SPA flyby with orbital angular momentum reversal. It should be noted that such a motion reversal is really difficult to be achieved by sailcraft with a cranking phase [3]. By using the high-performance sail concept, Vulpetti theoretically investigated two-dimensional [12] and three-dimensional H-reversal trajectories [13, 14]. The full theory of the reverse-motion solution to the general space sailing equations of motion, in particular the so-called fast-solar sailing, has been published in 2012 [15]. The most general trajectory related to SPS consists of arcs of direct motions and reverse-motion arcs separated by points where the orbital angular momentum reverses, not necessarily by vanishing.

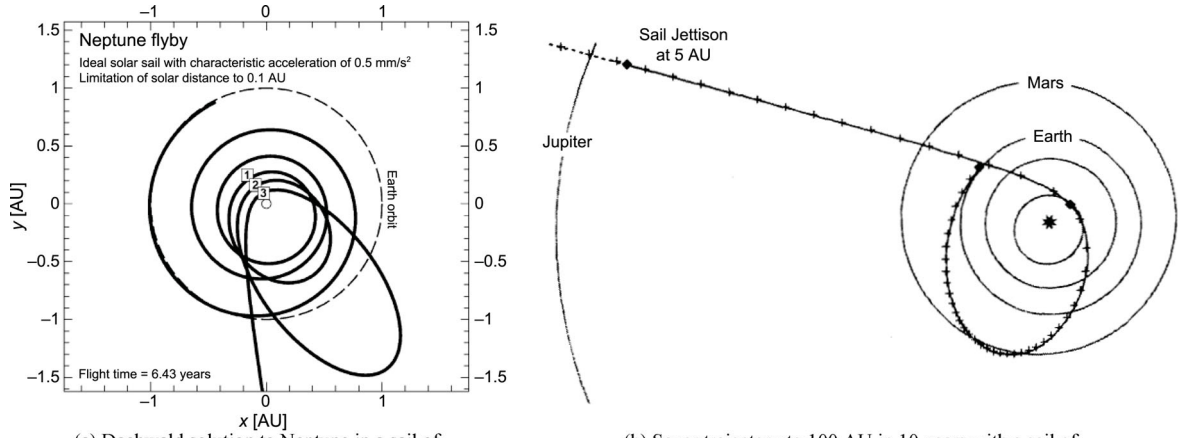

(a) Dachwald solution to Neptune in a sail of 0.5 mm/s² with a SPA of 0.1 AU. Reproduced with permission from Ref. [9], © American Institute of Aeronautics and Astronautics, Inc. 2004

(b) Sauer trajectory to 100 AU in 10 years with a sail of 2.4 mm/s² and 0.3 AU flyby. Reproduced with pemission from Ref. [3], © Univelt, Inc. 1999.

Fig. 1 Optimized solar sail trajectories to outer solar system with SPA flybys.

With the progress of scientific research on solar sails as well as engineering technology, studies on interstellar missions and high-performance sails have been increasing in the past decade. Dandouras, Pirard and Prado [16] investigated linear trajectories and heliostationary missions by using high performance sails. Lyngvi [2] made a technological reference study for heliopause probe missions. Zeng *et al.* [17] found the lowest characteristic acceleration to achieve the H-reversal model with constant sail attitudes. Follow-up studies [18] obtained a type of heliocentric periodic orbits in double H-reversal modes with fixed sail attitudes of half period. Extended results [19] were also obtained by analyzing time-optimized H-reversal periodic orbits. In 2017, Pino and Circi [20] studied the capture maneuver in the Alpha Centauri star system by adopting the H-reversal trajectory concept and considering the time-varying zero velocity curves.

In the context of this paper, a major encouragement comes from one of the *Cosmic Studies* originated, accomplished, and published by the International Academy of Astronautics (IAA, Paris–France) [21], and presented by author Vulpetti at the 8th IAA symposium on "The future of the space exploration: Towards the Stars" (July 2013, Turin, Italy). The related IAA Study Group has recommended that only two space propulsion types appear reliable and proper to IPMs: (a) SEP/NEP, and (b) Solar-Photon Sailing.

This paper is organized as follows: Section 2 reports some features of the H-reversal trajectory family. Some other applications of the H-reversal trajectory solution will be detailed in Section 3; this section consists of four subsections 3A through 3D according to as manyt mission classes. Section 4 is devoted to some important features of the three-dimensional motion-reversal trajectories. Concluding remarks can be found in Section 5.

2 Some characteristics of the family of H-reversal trajectories

A typical H-reversal trajectory starts from the Earth orbit as shown in Fig. 2(a). Zero hyperbolic excess velocity is usually assumed indicating that the sailcraft is directly inserted into a heliocentric orbit. To guarantee a 2D motion on the ecliptic plane, the sail surface (assumed flat on average) should be perpendicular to the ecliptic plane. Usually, two attitude angles are used to describe the orientation of a solar sail, i.e., the cone angle α and the clock angle δ shown in Fig. 2(b) [7], though another pair of angles could be appropriate [5]. The trajectory in Fig. 2(a) is obtained with prefixed angles $(\alpha,\ \delta) = (25.9°,\ 180°)$. With sail loading (i.e., sailcraft mass divided by sail area) of 2 g/m^2, the characteristic acceleration would be 4.5 mm/s^2 for an ideally reflecting sail orthogonal to the local sunlight direction, i.e., with thrust efficiency equal to 1. However, the non-ideal sail (Aluminum and Chromium on Kapton, 20 nm in roughness) of this example shows thrust efficiency of about 76 percent at 25.9° of sail pitch. With respect to the heliocentric inertial frame (HIF), the sail normal vector $\boldsymbol{n}$ appears changing with time; however, in the

sailcraft's heliocentric orbital frame, $\boldsymbol{n}$ is unchanged, and then easier to control and optimize.

The thrust acceleration in this example has been computed by using the scalar scattering theory of Optics applied to space sailing [13–15], which gives vector thrust values somewhat different from those ones obtained by assuming a perfectly-reflecting sail.

Originally, the aim of the H-reversal trajectory was to obtain as high an escape speed as possible; let us explain Fig. 2(a) in some details. In its initial phase, the orbital speed decreases by achieving the minimum at the point P shortly after the aphelion M. The sailcraft's projected orbital angular momentum (per unit mass), or $\mathbf{H}\cdot\boldsymbol{k}\equiv H$($\boldsymbol{k}$ denoting the direction of the z-axis of HIF) decreases gradually until it vanishes at point Q, where the orbital (vector) velocity points exactly to the Sun. If the sail were jettisoned at this point, a linear heliocentric arc falling directly into the Sun would be obtained [22]. After Q, the orbit is smoothly changed to the clockwise motion with a negative value of H; note that, by definition, the z-axis of HOF is the opposite of $\mathbf{H}$ after Q in the motion-reversal theory [15]. As the sailcraft approaches the Sun, the orbital energy increases to zero at point S: if the sail were jettisoned here, the gross payload would continue on a parabola. Differently from a classic Keplerian orbit, the maximum speed is achieved at point W, about five days after the perihelion point U. From about 7.5 AU on, the numerical analysis shows that there exists a speed plateau, which one can identify with a (long) cruise phase with speed practically constant. This behavior results from the combined actions of the transversal/radial lightness numbers and gravity [15]. No such feature can be obtained by gravity only. The final cruise speed is about 14.75 AU/yr, or 70 km/s, in this case. Fig. 2(a) also suggests us that some in-situ observations during the pre-perihelion phase are not only possible, but also new applications to space science could be conceived.

After this short introduction, a simplified theoretical derivation is given here below to show a few of the dynamical properties of H-reversal trajectories. Neglecting planetary disturbances in the two-body problem, the equations of motion of a sailcraft in HIF can be written as

$$\begin{aligned}
&\dot{\boldsymbol{r}}=\boldsymbol{v},\qquad \dot{\boldsymbol{v}}=-\frac{\mu}{r^3}\boldsymbol{r}+\boldsymbol{f}\\
&\boldsymbol{f}=\frac{\mu}{r^2}\beta\cos^2\alpha\left[\cos\alpha,\sin\alpha\cos\delta,\ \ \sin\alpha\sin\delta\right]^{\mathrm{T}}\\
&\quad\equiv\frac{\mu}{r^2}\zeta,\quad \zeta=\left[\zeta_{\mathrm{r}},\ \zeta_{\mathrm{t}},\ \zeta_{\mathrm{n}}\right]^{\mathrm{T}},\ \zeta_{\mathrm{r}}\geqslant 0\\
&\alpha\in[0,\ \pi/2],\ \delta\in[0,\ 2\pi)
\end{aligned}\tag{1}$$

Equations (1) are particularly simple, but notable, mainly because an ideally-reflecting flat surface has been assumed in the current framework. An ideal sail works as a reference for comparing real-sail results. Note that $\|\zeta\|=\beta\cos^2\alpha$. An extended explanation (and related mathematical models) of the many effects a sailcraft undergoes in the real world can be found in Ref. [5]

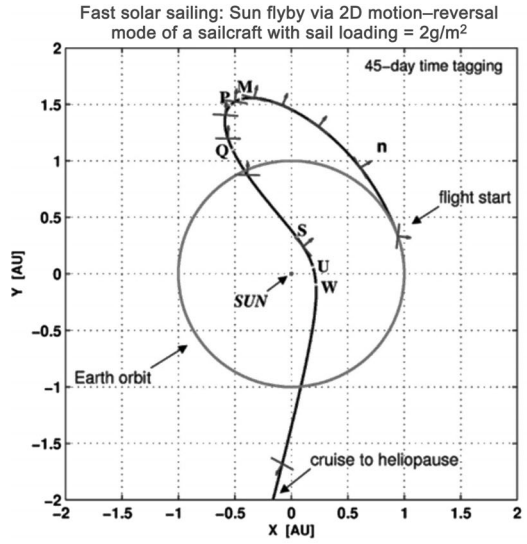

(a) An example of H-reversal trajectory

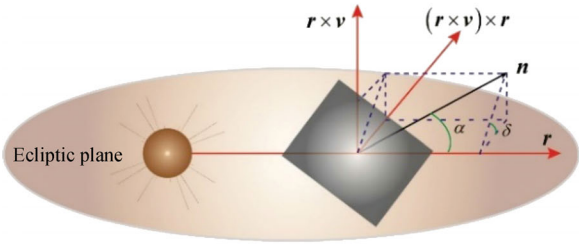

(b) Reference frame and sail attitude angles

Fig. 2 Solar sail H-reversal trajectory and definitions of sail attitude angles for 2D motion. Note: The orbital plane spanned by $\boldsymbol{r}$ and $\boldsymbol{v}$ coincides with the ecliptic plane for the 2D case.

and, primarily, in Ref. [15]. β is a very important parameter known as the sailcraft lightness number, from which the characteristic acceleration depends. Vector $\boldsymbol{\zeta}$ is the ideal-mirror case of the generalized lightness vector $\mathbf{L}$ [15], a (complicated) key quantity for expressing the thrust acceleration induced by electromagnetic waves on any flat element of a metal sail. In Ref. [15], the three dimensionless components of $\mathbf{L}$, and consequently those of $\boldsymbol{\zeta}$ here, are called the radial number, the transversal number, and the normal number, respectively. If β were exactly one, and if this ideal sail surface were perpendicular to the local sunlight direction, the (maximum) sail acceleration at 1 AU would be (very close to) 5.93 mm/s, namely, the solar gravitational acceleration of a test body at 1 AU. As for the other symbols in Eqs. (1), μ is the solar gravitational constant having the value of 1.3271244×10^{11} km^3/s^2, $\boldsymbol{r}$ and $\boldsymbol{v}$ denote the vector position and velocity, respectively, of the sailcraft, and $r = \|\boldsymbol{r}\|$ is the sail's heliocentric distance. Thus, $\boldsymbol{f}$ expresses the SRP-induced acceleration on the sail.

For 2D trajectories lying on the ecliptic plane, Equations (1) can be simplified by polar coordinates to give

$$\begin{aligned} \ddot{r} - r\dot{\theta}^2 + \frac{\mu}{r^2} &= \frac{\mu}{r^2}\left(\beta cos^3\alpha\right) = \frac{\mu}{r^2}\zeta_{\mathrm{r}} \\ \frac{1}{r}\frac{\mathrm{d}}{\mathrm{d}t}\left(r^2\dot{\theta}\right) &= \frac{\mu}{r^2}\left(\beta\cos^2\alpha\sin\alpha\right) = \frac{\mu}{r^2}\zeta_{\mathrm{t}} \end{aligned} \tag{2}$$

where θ is the sailcraft's polar angle in HIF considered at the flight epoch. Because $\delta = 0$ or π, it is more convenient to use one angle α in the range $[-\pi/2, \pi/2]$. From a strict mathematical viewpoint, there is no closed-form solution to Eqs. (2) if $\zeta_{\mathrm{t}} \neq 0$. Nevertheless, many notable properties can be inferred from this system of equations. Particularly important for our aims are the sailcraft's orbital energy, say E, and the time rate of the orbital angular momentum, i.e., $\boldsymbol{r}\times\boldsymbol{v} = \mathbf{H} \equiv H\boldsymbol{h}$, where the unit vector $\boldsymbol{h}$ is the z-axis of the heliocentric orbital frame defined such that $\boldsymbol{h}\cdot\boldsymbol{k} > 0$ independently of the direct or retrograde motion of the sailcraft; thus, the quantity H can have any sign. Of course, $|H| = \|\mathbf{H}\|$. By simple algebra, one can get

$$\begin{aligned} E &= \frac{1}{2}\|\boldsymbol{v}\|^2 - (1-\zeta_{\mathrm{r}})\frac{\mu}{r} \\ \dot{H} &\equiv \frac{\mathrm{d}H}{\mathrm{d}t} = \beta\frac{\mu}{r}\cos^2\alpha\sin\alpha = \frac{\mu}{r}\zeta_{\mathrm{t}} \end{aligned} \tag{3}$$

The energy equation shows that a solar-photon sailcraft 'senses' the Sun with an effective gravitational mass $\tilde{\mu} = (1-\zeta_{\mathrm{r}})\,\mu$; therefore, if one requests a solar flyby with a perihelion *lower* than that of the initial (osculating) orbit of the sailcraft, the first necessary condition is to have a sufficiently high value of the radial number, but not too high otherwise one would get an initial energy value $E_0 \geqslant 0$.

The second necessary condition for flyby is to decrease H until zero [15]; the second equation in Ref. (3) tells us that we must adopt a value of α in the interval of $(-\pi/2, 0)$, or $\zeta_{\mathrm{t}} < 0$, sufficiently high in absolute value to avoid an inward spiral. In the context of the current paper, we skip strict mathematical analysis and proceed towards potential applications. If we fix $\beta = 0.765$ and give α three appropriate values, three typical types of H-reversal trajectories can be obtained as shown in Fig. 3(a). Trajectories with perihelion distances in the 0.25–0.4 AU range are appropriate

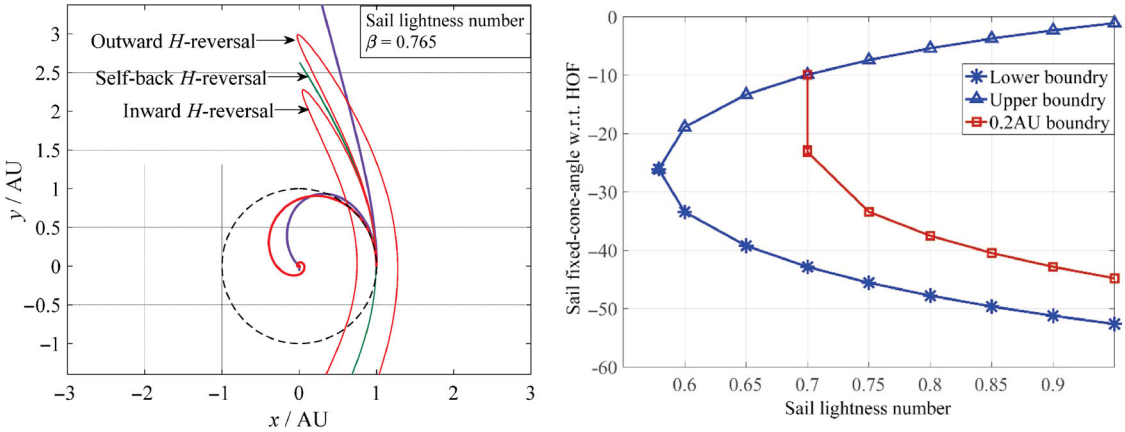

(a) Different types of H-reversal orbits (b) Feasible region of H-reversal orbits

Fig. 3 Different H-reversal trajectories and their feasible regions with fixed-attitude-angles. Reproduced with permission from Ref. [17], © Science China Press and Springer-Verlag Berlin Heidelberg 2011.

for IPMs with relatively high cruise speeds. It is interesting the existence of a self-back trajectory as a single curve crossing its starting point [17]. The feasible regions for H-reversal trajectories with different values of α and β are given in Fig. 3(b) via the hodograph method, where the region related to the perihelion of 0.2 AU is remarkable for future missions. The lower boundary marked with '$*$' and the upper boundary marked with 'Δ' represent boundary values for the fixed sail attitude angle to accomplish H-reversal motions. If the minimum distance is restricted to 0.2 AU, the magnitudes of lower boundary values are further reduced. For other orbital problems related to 2D H-reversal trajectories, the general feasibility region can be found in Chapter 7 of Ref. [15].

3 Applications of the H-reversal trajectory

In this section, few potential applications of the H-reversal trajectory are summarized to show recent progress. A first point consists of novel interstellar missions in H-reversal mode. The second point is about the newly-found heliocentric periodic orbits by using high-performance solar sails. A third point regards intercept trajectories and heliocentric transfers. Heliocentric transfer trajectories to elliptic rectilinear orbits by the H-reversal mode are also summarized. These potential applications have enhanced the theoretical research into the H-reversal trajectory family, which enforces new utilization of solar sail in the medium/long term.

3.1 Novel interstellar trajectories

To obtain the minimum time optimal solutions of H-reversal trajectories, we use the following objective function

$$J = -\int_0^{\mathrm{T}} \mathrm{d}t \approx -\int_0^{t_f} \mathrm{d}t \tag{4}$$

where T is the total flight time to the minimum target distance such as 200 AU. However, such a calculation may be simplified by assuming sail jettisoning, e.g., at 5 AU, which is considered by JPL [3], but not pursued by NASA/MSFC for not losing the propulsive increment of speed after 5 AU, some 7-8 percent, at least, especially at low mass-on-area ratio [5]. Thus, an approximate objective function with final time t_f to arrive at 5 AU is adopted, which is the same in Ref. [3].

Of the two general methods to solve optimal control problems, i.e. the direct or indirect methods, here we have used the Pontryagin's maximum principle. The time optimal control problem results in a two-point boundary value problem, which can be solved by using an improved shooting method [23, 24]. In our simulations, a sail with a characteristic acceleration of 4.5 mm/s^2 (lightness number 0.76) is utilized. Converged solutions have been given in Fig. 4 by summarizing corresponding orbital data in Table 1 [25].

Some considerations about direct motion and reversal motion solutions to the general SPS equations are in order. One should be careful to compare these two typical trajectories. Generally, an unconstrained optimal control performs better than a constrained control, as it is well known. Thus, in the current case of minimum flight time, one may (hastily) conclude that direct solar flybys are always better solutions with the same initial conditions compared to the H-reversal trajectories. This claimed conclusion is a misconception indeed. As a point of fact, the constant-sail-attitude H-reversal solution to the SPS equations of motion focuses on the simplicity of sail attitude control without degrading the dynamical output of the sailcraft. In contrast to what it might be though, H-reversal trajectories can be optimized with simple time-varying attitude profiles [26]. Furthermore, we have to remind the reader that even the Pontryagin's maximum principle is not able to provide solutions to *singular* control problems; to optimize SPS trajectories *is* a singular problem in terms of lightness vector, as explained strictly in Chapter. 8 of Ref. [15], so that one should switch to Non-Linear Programming, especially

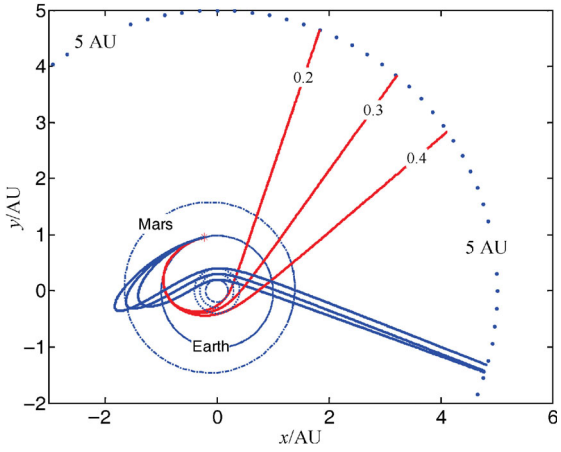

Fig. 4 Interstellar probe trajectories by a sail with 4.5 mm/s^2 in optimized sail attitude angles. Reproduced with permission from Ref. [25], © American Astronautical Society 2014.

Table 1 Time optimal results by an ideal-sail spacecraft with loading 2 g/m^2. ra denotes the aphelion distance whereas rp is the perihelion distance. Reproduced with permission from Ref. [25], © American Astronautical Society 2014.

r_{p} [AU]	Direct flybys				Reversal flybys			
	r_{a}[AU]	v_f[AU/yr]	t_f[yr]	$t_{250\mathrm{AU}}$[yr]	r_{a}[AU]	v_f[AU/yr]	t_f[yr]	$t_{250\mathrm{AU}}$[yr]
0.2	1.011	19.334	0.685	13.357	1.408	16.679	1.193	15.882
0.3	1.011	15.361	0.747	16.697	1.640	13.393	1.496	19.790
0.4	1.010	12.935	0.803	19.743	1.847	11.459	1.778	23.158

for particularly complicated SPS problems.

An example is now in order. In the 0.2 AU perihelion scenario, the flight time is 15.88 years to arrive at 250 AU. For the case of constant sail attitude angles of Fig. 2(a), the flight time can be estimated as 18 to 19 years for a speed of 14.75 AU/yr at the sail jettisoning. An increase of up to 3 years in flight time can be traded off with the simple constant-angle sail attitude that would guarantee the sail control throughout the mission.

For the considered challenging mission class, it appears reasonable that H-reversal trajectories with constant (but optimized) sail angles in HOF allow more reliable and realizable mission than what the unconstrained variable-attitude time-optimal solutions may do. Of course, with the development of new materials via nanotechnology, the flight time might be reduced in general by further decreasing the sailcraft sail loading. Some other interesting scenarios were also proposed with dual-sail sailcraft, which are described in Refs. [27, 28].

Above all, the direct and reversal motion solutions are not conflicting one another; in many cases, considering both in mission design would double the launch opportunities, and fast missions to the outer solar systems and beyond are an excellent example of that, appear technologically feasible and cost effective.

3.2 Heliocentric periodic orbits

Heliocentric periodic orbits are a natural extension of the H-reversal motion solution; instead of having one reversal point, many of them build new families of heliocentric orbits. The existence of many-arc trajectories with direct-motion and reversed-motion is admitted by the theory about the most general SPS trajectory type [15]. In a heliocentric periodic orbit driven by solar sail, the sailcraft departure position is exactly on the axis ox as shown in Fig. 5(a); the orbit is symmetrical with respect to the axis ox and faces one side of the Sun. Thus, its orbital perihelion point is also on the positive the axis ox, and consequently, only half periodic orbit is sufficient to be analyzed [18]. The conditions for such planar orbits are specified as

$$[x_p \quad y_p \quad v_{px}]^{\mathrm{T}} = [r_p \quad 0 \quad 0]^{\mathrm{T}} \tag{5}$$

where the subscript 'p' denotes the perihelion point. The

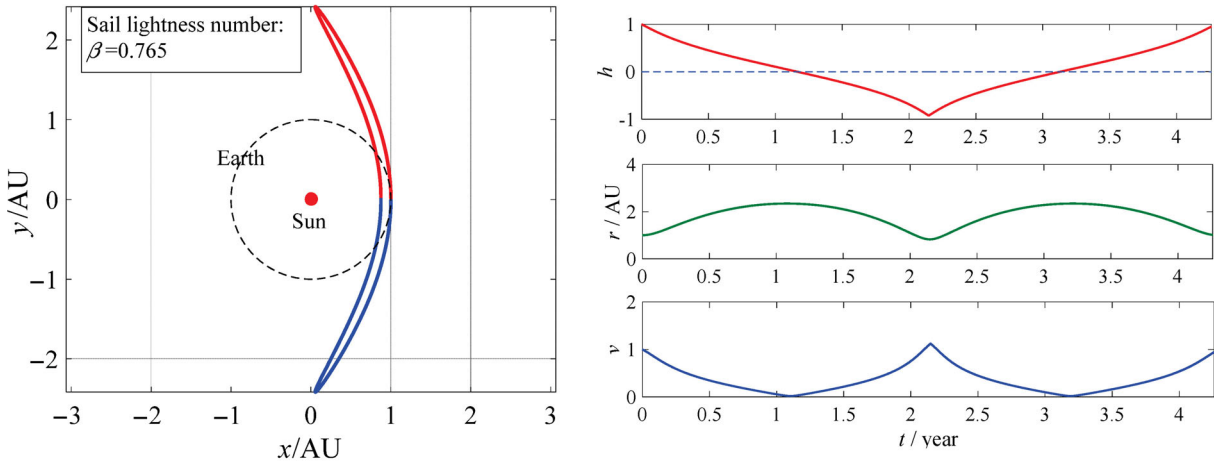

(a) H-reversal periodic orbit (b) Variational profile of system variables

Fig. 5 Heliocentric periodic orbit with H-reversal model and history of orbit variables. Reproduced with permission from Ref. [18], © *Journal of Tsinghua University (Science and Technology)* 2012.

variables x_p, y_p are the x-coordinate and y-coordinate of the perihelion, respectively, v_{px} denotes the magnitude of orbital velocity along the axis ox, and r_p is the Sun-sailcraft distance. Note that for each half period of the orbit, the required sail attitude is fixed with respect to the heliocentric orbital frame.

A set of dimensionless units is used in the numerical simulations listed in Table 2: The unit distance is set to be 1 AU, and the unit speed is taken to be the same as the (ideal) Earth mean orbital speed. With such units, the Earth orbits the Sun within a period of 2π. When the sail lightness number is 0.765 (i.e., a characteristic acceleration of 4.5 mm/s^2 with perfect reflection again), the periodic H-reversal orbit is obtained in Fig. 5(a) where for simplicity the Earth orbit is assumed as 1 AU circular orbit. Fig. 5(b) illustrates the variational profile of the orbit variables, which are the orbital angular momentum h, the orbital radius r, and the orbital velocity v. One can note that the direction of h changes twice in one period. The orbital period is about 8.52π, or 4.26 yr, driven by a constant sail pitch angle of $-20.52°$.

For the constant-angle cases, the number of H-reversal periodic orbits is finite as there is only one solution for each pair of lightness number and cone angle. To enrich families of H-reversal periodic orbits, a time-optimal control model can be introduced with time-varying cone angles [18]. The constraint at the perihelion point can be expressed as

$$\begin{aligned}&\boldsymbol{\Phi}_p\left[t_p,\ \boldsymbol{R}(t_p),\ \boldsymbol{V}(t_p)\right]=\\&\left[x(t_p)-x_p,\ y(t_p),\ z(t_p)-z_p,\ v_x(t_p),\ v_z(t_p)\right]^{\mathrm{T}}=0\end{aligned}\tag{6}$$

To maximize the objective function $-\lambda_0\int_0^{t_p}\mathrm{d}t$, where λ_0 is a positive constant, the corresponding Hamiltonian is

$$\mathbb{H}_s=-\lambda_0+\boldsymbol{\lambda}_{\mathbf{R}}(t)\cdot\boldsymbol{V}+\boldsymbol{\lambda}_{\mathbf{V}}(t)\cdot\left[-\frac{1}{R^3}\boldsymbol{R}+\beta\frac{1}{R^4}(\boldsymbol{R}\cdot\boldsymbol{n})^2\boldsymbol{n}\right]\tag{7}$$

where the dynamical equations are the same as Eq. (1) (but in dimensionless units), and $\boldsymbol{\lambda}_{(.)}$ are Lagrange multipliers. The optimal sail attitudes are obtained by maximizing $\mathbb{H}_s$ (which is distinguished from the magnitude of the orbital angular momentum H) at any time in the following equation as

$$\boldsymbol{n}(t)=\arg\max\mathbb{H}_s\left(t,\boldsymbol{n},\boldsymbol{\lambda}_{(.)}\right).\tag{8}$$

As for solar sails, the optimal orientations are different from conventional high-thrust systems or continuous low-thrust rocket systems. To satisfy Eq. (8), the sail normal vector $\boldsymbol{n}$ must be directed to obtain the largest projection on the (time-variable) primer vector $\boldsymbol{\lambda}_{\mathbf{V}}$; that results in

$$\boldsymbol{n}=\begin{cases}\dfrac{\sin(\tilde{\alpha}-\alpha)}{\sin\tilde{\alpha}}\dfrac{\boldsymbol{R}}{\|\boldsymbol{R}\|}+\dfrac{\sin\alpha}{\sin\tilde{\alpha}}\dfrac{\boldsymbol{\lambda}_{\mathbf{V}}}{\|\boldsymbol{\lambda}_{\mathbf{V}}\|}, & \tilde{\alpha}\in(0,\pi)\\[2ex] \dfrac{\boldsymbol{R}}{\|\boldsymbol{R}\|}=\hat{\boldsymbol{r}}, & \tilde{\alpha}=0\end{cases}\tag{9}$$

where $\tilde{\alpha}$ is the angle between the primer vector and $\hat{\boldsymbol{r}}$. For a detailed discussion about the optimization method and its solving algorithm, one can read Ref. [18]. Also, there are some locally time-optimal solutions which have been addressed in Ref. [10].

Figure 6 shows an example of time-optimal H-reversal periodic orbit in the ecliptic plane. The lightness number is 0.6 and the perihelion is set to be 0.2 AU. Two different aspects should be noted compared to the constant-angle interstellar precursor trajectory of Fig. 2(a). The first one is the time-varying attitude as shown in Fig. 6(b). Second, a rapid cone-angle control is required around perihelion. Similar type of orbits was carried out by minimizing the sail characteristic acceleration in Ref. [29].

Three-dimensional H-reversal periodic orbits can be also obtained. For instance, we have considered $\beta=0.7$ and the constraints $x_p=0.2$ AU, $z_p=0.0$ AU, and $0\leqslant z\leqslant 0.5$ AU that resulted in the trajectory projections on the three coordinate planes as shown in Fig. 7 [30]. Such trajectories may be utilized for periodic observations of the interplanetary environment, especially around each aphelion. The class of H-reversal periodic orbit family is not limited to two reversal points per orbit. In Ref. [31], orbits exhibiting four orbital angular momentum reversals have been analyzed;

Table 2 Dimensionless (solar) units

Length (AU)	Velocity	Time
1.4959787×10^{11} m	2.924×10^{4} m/s	5.022×10^{6} s

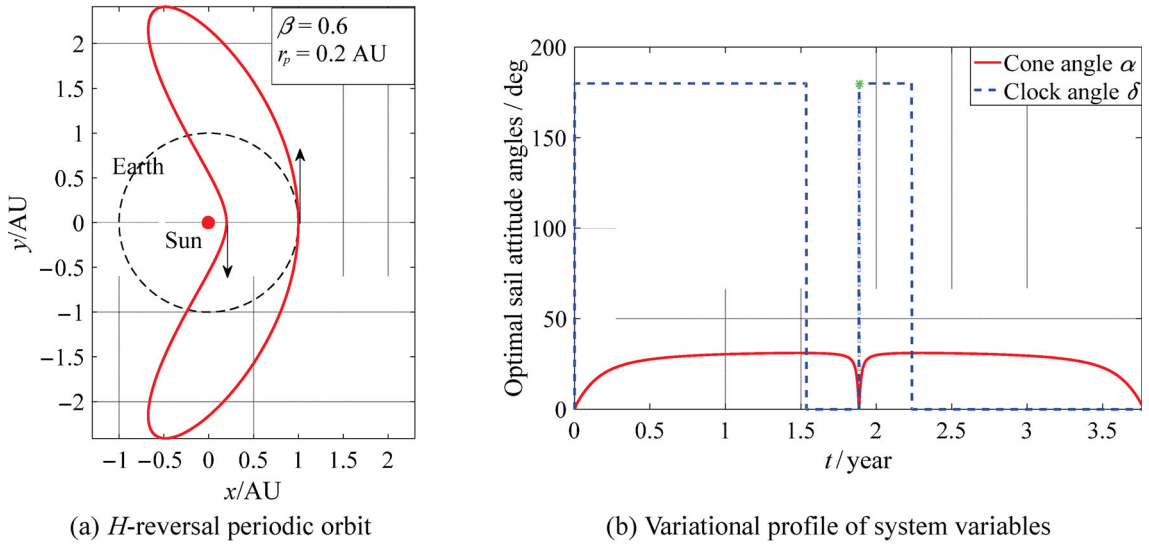

(a) H-reversal periodic orbit (b) Variational profile of system variables

Fig. 6 Time-optimal H-reversal periodic orbit and profile of sail orientations. Reproduced with permission from Ref. [19], © RAA 2011.

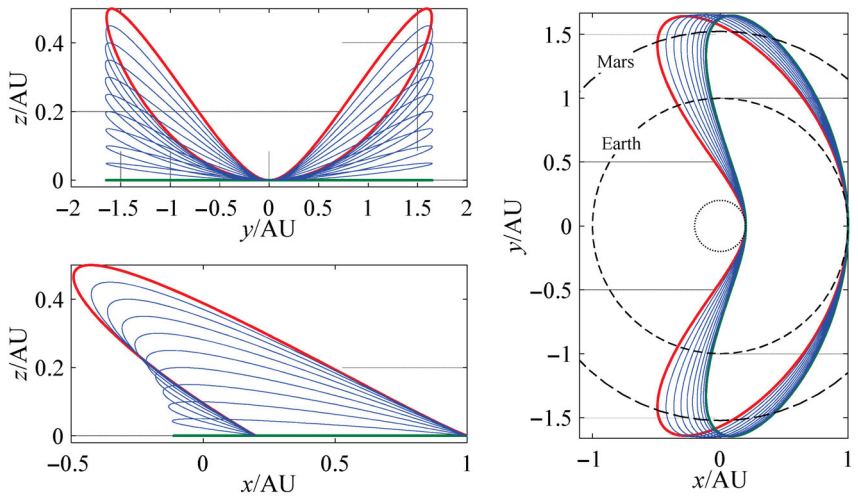

Fig. 7 Double H-reversal periodic orbits in the 3D space. Reproduced with permission from Ref. [30], Springer Science + Business Media B.V. 2011.

in particular, each orbital cycle is characterized by two quasi-heliostationary conditions near the reversal points.

3.3 Asteroid deflection with H-reversal intercepting trajectories

As a further application, Zeng *et al.* [18] have proposed to carry out heliocentric transfers by using H-reversal trajectories. Like the above H-reversal periodic orbits, a clockwise periodic orbit can be obtained by jettisoning the sail at the perihelion. One could design a mission with the perihelion velocity to obtain a circular orbit about the Sun. In particular, if a 3D H-reversal is used, a displaced solar orbit can be obtained right above or below the Sun for valuable close-up view of the solar polar regions.

The focus of this section is an intercept trajectory by solar sail in the H-reversal mode. Zeng *et al.* [18] proposed head-on impact on deflecting a dangerous asteroid away from its original orbit in order to avoid collision between the asteroid and the Earth. Both 2D and 3D cases were discussed based on numerical simulations by taking the asteroid 99942 Apophis as an example. An extended study was made by Gong *et al.* [32] within realistic orbital elements of the Earth and Apophis to carry out an appropriate head-on impact.

Note that the physical size of the asteroid [33] and the sailcraft are neglected in the aforementioned studies, where only particle dynamics is considered.

Figure 8 illustrates some intercepting trajectories by SPAs to deflect a hypothetical near-Earth asteroid. The Earth orbit assumed as 1 AU circular orbit can be taken as a reference for the scale of optimized trajectories, where the perihelion distance of SPA flybys is 0.4 AU. Compared to slow-push strategies such as the gravitational tractor, kinetic impacting spacecraft should be one of the most feasible methods to implement asteroid deflection missions [34, 35]. It appears that H-reversal trajectories with head-on impacting would be better than the direct SPA flybys to achieve more colliding energy. On such a basis, a comparison study was made by assuming a circular orbit for the target asteroid. Numerical results show that direct SPA flybys are superior to the H-reversal trajectories in both flight time and final impacting speed [36]. However, again, such a conclusion does not take the sail's continuous attitude control difficulties into account. From an engineering point of view, to design a trajectory with (a small number of) piecewise attitude control arcs in HOF is much easier to be implemented, and affects the other sailcraft systems more advantageously so that, ultimately, the cost of the whole sailcraft is greatly reduced.

Finally, although not yet analyzed quantitatively, the H-reversal strategy should allow performing a rendezvous with a retrograde comet without using the cranking phase [3]; this motion-reversal advantage would come from the need of turning over the initial direct-motion orbit plane like the sailcraft orbit inclination change of about 125° (lasting 421 days) in the JPL's famous solar-sail mission concept in the 1970s [37]; that concept aimed at a rendezvous with the Halley comet during its return in the 1986. Next solar close encounter of this comet will be in 2061.

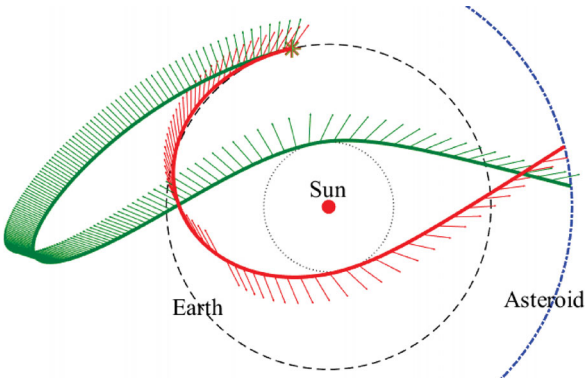

Fig. 8 Asteroid intercepting trajectories as computed. Reproduced with permission from Ref. [36], © IEEE 2014. Each side fringe on each example trajectory denotes the direction of the sail backside normal $\boldsymbol{n}$ as would observed in HIF.

3.4 Transfer trajectories to elliptic rectilinear orbits

An elliptic rectilinear orbit is a special trajectory, where the ellipse degenerates into a line segment connecting both foci. It is a limit case for the elliptical orbit whose semi-major axis is in a finite value with an eccentricity of unity. Such orbits can be applied to understand dynamical behaviors of cometary bodies whose eccentricity is close to unity [38]. They might be also used by scientific probes to approach the Sun, and obtaining in-situ observations of the solar wind, solar gravitational harmonics, and interstellar dust too, just to cite a few [39]. Due to the massive fuel consumption of transfer trajectories via rocket, rectilinear orbits were rarely discussed for scientific missions. In 2004, Dandouras *et al.* [16] proposed a two-probe scientific mission concept where the second probe is released to free-falling into the Sun along a rectilinear orbit. Initially, the spacecraft should be in a heliostationary orbit at a fixed position with characteristic sail accelerations a_c not less than the solar gravitational attraction [15]. In 2011, Quarta and Mengali [40] investigated the capability of a solar-sail spacecraft to reach an elliptic rectilinear orbit for which the value of a_c is less than the solar gravitational acceleration, namely, the lightness number is less than unity. The transfer trajectory is essentially a segment of an H-reversal trajectory until the orbital angular momentum vanishes.

A typical rectilinear orbit and its transfer trajectory by using solar sail is shown in Fig. 9(a). A sailcraft departs from the Earth orbit with zero hyperbolic excess velocity at point D. The transfer phase develops up to the point Q, which is set to be the same as given in Fig. 2(a). At the point Q, the sail is jettisoned to fully deploy the scientific probe. The rectilinear phase ranges from Q to the ending point E, where the solar probe is destroyed by the solar environment. In order to get a long mission time of the rectilinear phase, one needs a distant r_{Q}. On the other hand, instead of sail jettison at

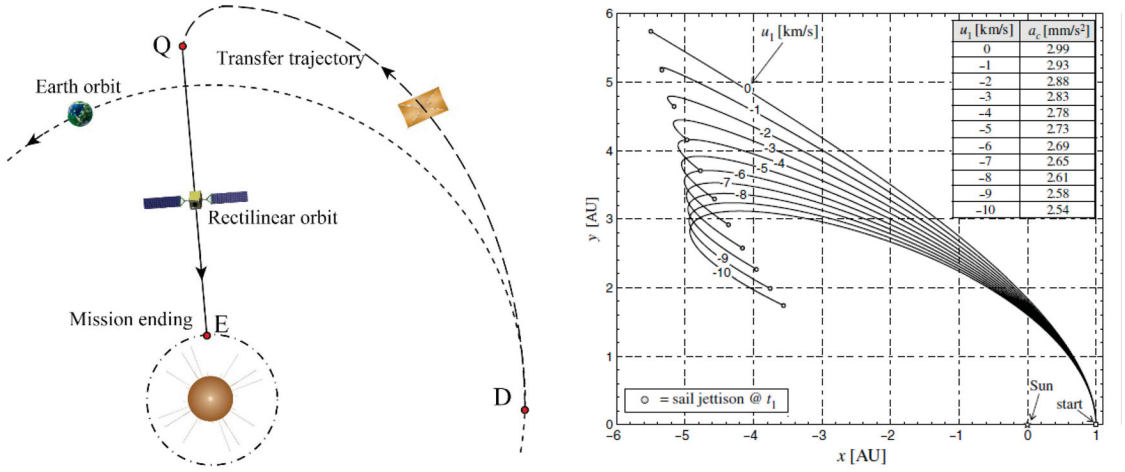

(a) Sketch map for an elliptic rectilinear orbit

(b) H-reversal transfer trajectories. Reproduced with permission from Ref. [40], © Elsevier Ltd. 2012.

Fig. 9 Heliocentric elliptic rectilinear orbit and its transfer trajectories by solar sail.

the point Q, if the sail is oriented radially, the original mission time for QE phase will be further extended depending on the sail capacity. In that case the sail acceleration is against the solar gravitational attracting. If the sail lightness number is equal or greater than unity, a heliostationary orbit may be achieved with zero velocity at the H-reversal point Q [16].

A type of optimal transfer trajectories was obtained by Quarta and Mengali by minimizing the acceleration a_c [40]. With a prefixed transfer time and a given radial velocity at point Q pointing to the Sun, a family of transfer trajectories were obtained as shown in Fig. 9(b). It was found that by increasing the magnitude of the radial speed at point Q from 0 km/s to 10 km/s, the value of a_c decreases from 2.99 mm/s^2 to 2.54 mm/s^2, respectively. In their simulations, an ideally-reflecting planar sail was assumed to departure from the 1 AU circular orbit with zero hyperbolic velocity. Such trajectories were extended to 3D cases too by using a piece-wise constant steering law [40]: rectilinear orbits could surely be reached by using H-reversal trajectories with sail's constant attitude in HOF. A detailed analysis on H-reversal heliocentric-transfer trajectories by using solar sails can be found in Ref. [22].

4 Further remarks on the existence of 2D and 3D motion reversal

In this paper, we have reported a few items from the rigorous treatment, made in Ref. [15] and mentioned in the above sections, about some key astrodynamical aspects of the motion-reversal based sailcraft missions. We refer mainly to the theorems and propositions in Chapter 7 of [15]. The above-described 2D H-reversal trajectories are obtained by zeroing the third component (or the *normal number*) of the lightness vector $\mathbf{L} \equiv [L_\mathrm{r},\ L_\mathrm{t},\ L_\mathrm{n}]^\mathrm{T}$ of which the vector $\boldsymbol{\zeta} \equiv [\zeta_\mathrm{r},\ \zeta_\mathrm{t},\ \zeta_\mathrm{n}]^\mathrm{T}$ in Eq. (1) is a particular case. (We remind the reader that $\mathbf{L}$ is always defined in HOF). If one tries to get a 3D motion-reversal trajectory by using constant $\mathbf{L}$ with $L_\mathrm{n} \neq 0$ for any finite time interval, no such a trajectory is possible (Lemma 7.1 of Ref. [15]), namely, one cannot obtain $\|\mathbf{H}\| = 0$ at any time, even conceptually, by this way. Thus, because controlling the sail attitude such that $L_\mathrm{n} = 0$, strictly, is unviable for a finite time, one might conclude that the elegant 2D H-reversal trajectories belong to the mathematical abstraction only, similarly to the perfect circular orbit, for example.

However, things are more complicated, and favorable at the same time. One should first note that the only way to smoothly reversing a (variable) vector, constrained to be orthogonal to a given plane, is to pass through the zero value. However, in the 3D space, an unconstrained variable vector can be reversed, for instance, with respect to the reference plane XY, by tilting it smoothly, crossing the XY plane, and reaching the opposite semi-space; there is no need to zeroing the vector length [41]. At the reversal point, $\mathbf{H}$ does not vanish as shown in Fig. 10, which is different from the aforementioned 2D case. This property of space

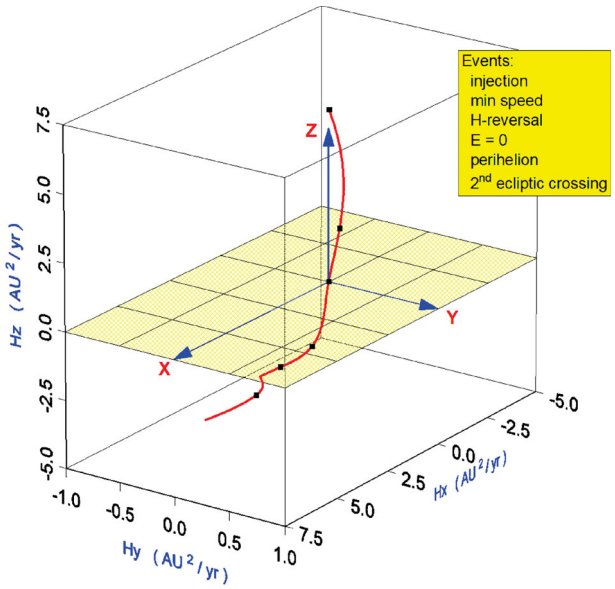

Fig. 10 Profile of the orbital angular momentum of a sample H-reversal trajectory in the HIF. Reproduced with permission from Ref. [41], © American Institute of Physics 2001. Flight begins with positive H_z. Special events are indicated.

is implicitly used to define a 3D regular trajectory arc where $\mathbf{H}$ reverses, and then give the related motion an unambiguous meaning (Definition 7.2 in Ref. [15]). This is a general definition that can be applied to any spacecraft, in principle.

Theorem 7.2 in Ref. [15] states a set of four conditions for a three-dimensional regular trajectory exhibits motion reversal at some instant. This set, as a whole, is sufficient for the existence of these trajectories; each of them admits *at least* one point where the motion reversal takes place. The set of the reversal points is a countable set. Combining these conditions with the properties of the 2D H-reversal motion results in the simplest sail attitude profile bringing about a (true) 3D motion-reversal trajectory. Put simply, this profile consists of three trajectory arcs (Chapters. 7–8 in Ref. [15]): (1) one arc starting from, say, t_0 to a certain instant t_1 with $\mathbf{L}^{(1)}$ = constant throughout $[t_0, t_1]$; (2) a second arc with $\mathbf{L}^{(2)}$ rotating about the X-axis of HOF from t_1 to t_2, and (3) a third arc from t_2 to t_f with $\mathbf{L}^{(3)}$ = constant again. In particular, one gets $\mathbf{L}^{(2)}(t_1) = \mathbf{L}^{(1)}$, $\mathbf{L}^{(2)}(t_2) = \tilde{\mathrm{U}}\mathbf{L}^{(2)}(t_1)$ (where $\tilde{\mathrm{U}}$ is a rotation matrix) with $L_\mathrm{t}^{(2)}(t_2) = -L_\mathrm{t}^{(2)}(t_1)$, and $\mathbf{L}^{(3)}(t_2) = \mathbf{L}^{(2)}(t_2)$. The second arc lasts much less than the other two arcs, in general, and contains the 3D reversal point, say, P$*$ at $t = t*$. The durations of the three arcs, the values of the two constant lightness vectors and the variable one, and the position $(\mathrm{P}*, t*)$ inside the second arc can be optimized quite a general way by a code based on the Non-Linear Programming method with linear and non-linear constraints. When more than one reversal points are admitted, a very wide variety of missions can be carried out. At each reversal point, the mentioned theorem 7.2 is strictly satisfied.

5 Conclusions and prospects

The family of the H-reversal trajectories has been revisited. This solar-photon sailing mode is very attractive for interstellar precursor missions. After a brief introduction about the solar sail propulsion and probe missions to the outer solar system and beyond, a detailed description of 2D H-reversal trajectories is given. The reversal of the orbital angular momentum is theoretically presented based on the planar dynamical equations of the heliocentric two-body problem. The workable regions for fixed-cone-angle H-reversal trajectories are also given.

Four main applications of the H-reversal trajectory have been summarized, including trajectories for escaping from the solar system, heliocentric H-reversal periodic orbits, interception trajectories for asteroid deflection, and transfer trajectories to reach elliptic rectilinear orbits. Also, rendezvous with a retrograde comet may be of great future interest. It is emphasized that a constant-attitude-in-HOF H-reversal trajectory is by far more advantageous in attitude control compared to the attitude control complexity related to the time-varying direct SPA flybys; substantially, one trades off a small surplus of flight time for a great attitude system simplicity and reliability, especially for the large surfaces of medium-term high-performance sails. Heliocentric periodic orbits with double H-reversal modes have been discussed. A simple comparison between direct SPA flybys and H-reversal flybys has been done for asteroid-intercepting missions.

In the near term, more applications of the H-reversal motion concept are expected with the rapid evolution of the sail technology. In any case, a next step could be to re-analyze the 2D H-reversal scenarios and mission concepts discussed in this paper by using the theorem mentioned and referenced in Section 4. This (original) investigation would eventually result in a realistic 3D motion-reversal family that, in turn, may act as the starting point for an actual mission design.

Acknowledgements

This work was supported by the National Natural Science Foundation of China (No. 11602019) and the Young Elite Scientist Sponsorship Program by CAST (2016QNRC001). The Excellent Young Teachers Program of Beijing Institute of Technology (2015YG0605) is acknowledged as well.

References

[1] Macdonald, M., McInnes, C., Hughes, G. Technology requirements of exploration beyond Neptune by solar sail propulsion. *Journal of Spacecraft and Rockets*, **2010**, 47(3): 472–483.

[2] Lyngvi, A., Falkner, P., Peacock, A. The interstellar heliopause probe technology reference study. *Advances in Space Research*, **2005**, 35(12): 2073–2077.

[3] Sauer, C. G. Jr. Solar sail trajectories for solar polar and interstellar probe missions. In: Proceedings of the AAS/AIAA Astrodynamics Specialist Conference, **1999**, 547–562.

[4] Johnson, L., Leifer, S. Propulsion options for interstellar exploration. In: Proceedings of the 36th AIAA/ASME/SAE/ASEE Joint Propulsion Conference and Exhibit, **2000**.

[5] Matloff, G. L., Vulpetti, G., Bangs, C., Haggerty, R. The interstellar probe (ISP): Pre-perihelion trajectories and application of holography. NASA/CR-2002-211730, NASA Marshall Space Flight Center, **2002**.

[6] Macdonald, M., McInnes, C. R. Solar sail mission applications and future advancement. In: Proceedings of the 2nd International Symposium on Solar Sailing, **2010**.

[7] McInnes, C. R. Solar sailing: technology, dynamics, and mission applications. Springer, **1999**.

[8] Leipold, M., Wagner, O. 'Solar photonic assist' trajectory design for solar sail missions to the outer solar system and beyond. In: Proceedings of the AAS/GSFC International Symposium on Space Flight Dynamics, **1998**.

[9] Dachwald, B. Optimal solar-sail trajectories for missions to the outer solar system. *Journal of Guidance, Control, and Dynamics*, **2005**, 28(6): 1187–1193.

[10] Zeng, X. Y., Li, J. F., Baoyin, H. X., Gong, S. P. Trajectory optimization and applications using high performance solar sails. *Theoretical and Applied Mechanics Letters*, **2011**, 1(3): 033001.

[11] Vulpetti, G. Missions to the heliopause and beyond by staged propulsion spacecrafts. In: Proceedings of the 43rd World Space Congress, **1992**.

[12] Vulpetti, G. Sailcraft at high speed by orbital angular momentum reversal. *Acta Astronautica*, **1997**, 40(10): 733–758.

[13] Vulpetti, G. 3D high-speed escape heliocentric trajectories by all-metallic-sail low-mass sailcraft. *Acta Astronautica*, **1996**, 39(1–4): 161–170.

[14] Vulpetti, G. General 3D H-reversal trajectories for high-speed sailcraft. *Acta Astronautica*, **1999**, 44(1): 67–73.

[15] Vulpetti, G. Fast solar sailing: astrodynamics of special sailcraft trajectories. Springer, **2013**.

[16] Dandouras, I., Pirard, B., Prado J. Y. High performance solar sails for linear trajectories and heliostationary missions. *Advances in Space Research*, **2004**, 34(1): 198–203.

[17] Zeng, X. Y., Baoyin, H. X., Li, J. F., Gong, S. P. Feasibility analysis of the angular momentum reversal trajectory via hodograph method for high performance solar sails. *Science China Technological Sciences*, **2011**, 54(11): 2951–2957.

[18] Zeng, X. Y., Baoyin, H. X., Li, J. F., Gong, S. P. A solar sail inverse periodic orbit. *Journal of Tsinghua University* (*Science and Technology*), **2012**, 52(1): 118–121. (in Chinese)

[19] Zeng, X. Y., Baoyin, H. X., Li, J. F., Gong S. P. New applications of the H-reversal trajectory using solar sails. *Research in Astronomy and Astrophysics*, **2011**, 11(7): 863–878.

[20] Pino, T., Circi, C. A star-photon sailcraft mission in the Alpha Centauri System. *Advances in Space Research*, **2017**, 59(9): 2389–2397.

[21] Bruno, C., Matloff, G. Key technologies to enable near-term interstellar scientific precursor missions. China Aerospace Publishing House, **2013**. (in Chinese)

[22] Quarta, A. A., Mengali, G. Solar sail capabilities to reach elliptic rectilinear orbits. *Journal of Guidance, Control, and Dynamic*, **2011**, 34(3): 923–927.

[23] Jiang, F. H., Baoyin, H. X., Li, J. F. Practical techniques for low-thrust trajectory optimization with homotopic approach. *Journal of Guidance, Control, and Dynamics*, **2012**, 35(1): 245–258.

[24] Pan, B. F., Lu, P., Pan, X., Ma, Y. Y. Double-homotopy method for solving optimal control problems. *Journal of Guidance, Control, and Dynamics*, **2016**, 39(8): 1706–1720.

[25] Zeng, X. Y., Alfriend, K. T., Li, J. F., Vadali, S. R. Optimal solar sail trajectory analysis for interstellar missions. *The Journal of the Astronautical Sciences*, **2012**, 59(3): 502–516.
[26] Wie, B. Sail flatness, attitude, and orbit control issues for an ST-7 solar sail spacecraft. In: Proceedings of the Solar Sail Technical Interchange Meeting, **2001**.
[27] Vulpetti, G. Reaching extra-solar-system targets via large post-perihelion lightness-jumping sailcraft. *Acta Astronautica*, **2011**, 68(5–6): 636–643.
[28] Zeng, X. Y., Alfriend, K. T., Vadali, S. R., Baoyin, H. X., Gong, S. P. Time-optimal trajectory design for a dual-satellite sailcraft interstellar mission with probe release (AAS 13–221). In: Proceedings of the 23rd Spaceflight Mechanics Meeting, **2013**.
[29] Mengali, G., Quarta, A. A., Romagnoli, D., Circi, C. H^2-reversal trajectory: a new mission application for high-performance solar sails. *Advances in Space Research*, **2011**, 48(11): 1763–1777.
[30] Zeng, X. Y., Baoyin, H. X., Li, J. F., Gong, S. P. Three-dimensional time optimal double angular momentum reversal trajectory using solar sails. *Celestial Mechanics and Dynamical Astronomy*, **2011**, 111(4): 415–430.
[31] Zeng, X. Y., Alfriend, K. T., Vadali, S. R. Solar sail planar multireversal periodic orbits. *Journal of Guidance, Control, and Dynamics*, **2014**, 37(2): 674–681.
[32] Gong, S. P., Li, J. F., Zeng, X. Y. Utilization of an H-reversal trajectory of a solar sail for asteroid deflection. *Research in Astronomy and Astrophysics*, **2011**, 11(10): 1123–1133.
[33] Zeng, X. Y., Gong S. P., Li J. F., Alfriend K. T. Solar sail body-fixed hovering over elongated asteroids. *Journal of Guidance, Control, and Dynamics*, **2016**, 39(6): 1223–1231.
[34] Pitz, A., Kaplinger, B., Vardaxis, G., Winkler, T., Wie, B. Conceptual design of a hypervelocity asteroid intercept vehicle (HAIV) and its flight validation mission. *Acta Astronautica*, **2014**, 94(1): 42–56.
[35] Vardaxis, G., Wie, B. Impact risk analysis of Near-Earth asteroids with multiple successive Earth encounters. In: Proceedings of the AAS/AIAA Space Flight Mechanics Meeting, **2016**.
[36] Zeng, X. Y., Gong, S. P., Li, J. F. Earth-crossing asteroid intercept mission with a solar sail spacecraft. *IEEE Aerospace and Electronic Systems Magazine*, **2014**, 29(10): 4–15.
[37] Wright, J. L. Space sailing. Gordon and Breach Science Publishers, **1993**.
[38] Roy, A. E. Orbital motion. In: Proceedings of the Institute of Physics Publishing, **2005**, 87–89.
[39] Colombo, G., Lautman, D. A., Pettengill, G. An alternative option to the dual-probe out-of-ecliptic mission via Jupiter swingby. In: Proceedings of the Symposium on the Study of the Sun and Interplanetary Medium in Three Dimensions, **1976**, 37–47.
[40] Quarta, A. A., Mengali, G. Optimal solar sail transfer to linear trajectories. *Acta Astronautica*, **2013**, 82(2): 189–196.
[41] Vulpetti, G. Sailcraft-based mission to the Solar Gravitational Lens. In: Proceedings of the AIP Conference Proceedings, **2000**, 504(1): 968–973.

Xiangyuan Zeng is an associate professor in the School of Automation, Beijing Institute of Technology. He received his Ph.D. degree of Mechanics from Tsinghua University, in 2013, and worked there as a postdoctor until 2015. He was ever a visiting scholar of Texas A&M University from 2011 to 2012, and a visiting professor in Sapienza University of Rome, in 2018, supported by the Young Elite Scientist Sponsorship Program by CAST (YESS). His current research interests are astrodynamics near asteroids, surface dynamics and bionic robots for surface explorations. E-mail: zeng@bit.edu.cn

Giovanni Vulpetti has received his M.S. and Ph.D. degrees, in 1969 and 1973, respectively. He specialized in astrodynamics, and wrote many tens of scientific papers about interstellar flight, astrodynamics and propulsion concepts, in particular the matter-antimatter annihilation propulsion. In 1979, he joined Telespazio SpA in Italy. From 1995 to 2013, he has been a member of the IAA committee for Lunar Base & Mars exploration. In 2001, he was a consultant at NASA/MSFC for studying the astrodynamics of NASA Interstellar Probe. He has implemented large computer codes for mission analysis and trajectory optimization via rockets and solar-sails. In 1990s, he contributed to the IAA committee for small satellites. As an application, he proposed and got the approval from Telespazio's CEO for the Telespazio's micro-satellite named TEMISAT, which launched in 1993, from the base Plesetsk in Russia. From 2006 to 2007, he worked for the company Galilean Plus S.r.l. in Italy as the chief scientist, where he contributed to the program of the Italian Space Agency. After that, he served as the guest managing editor of Acta Astronautica, in 2009 and

2014, respectively. Since 2013, he has been a senior guest lecturer at the Department of Astronautical Engineering of the Sapienza University of Rome. Since 1994, he has been a full member of the International Academy of Astronautics in France. E-mail: g.vulpetti.iaa@gmail.com.

Christian Circi is currently an assistant professor in flight mechanics at the Department of Astronautical, Electrical and Energy Engineering, Sapienza University of Rome. He got his M.S. degrees in aeronautical engineering and aerospace engineering, and pursued his Ph.D. degree in aerospace engineering at Sapienza University of Rome. He worked as a researcher at the Grupo de Mecanica of Vuelo-Madrid (GMV), and a research assistant at the Department of Aerospace Engineering. He is a lecturer in "Interplanetary Trajectories" and "Flight Mechanics of Launcher" in the master degree course of Space and Astronautical Engineering at Sapienza University of Rome. His principal research fields are: third-body and solar perturbations, interplanetary and lunar trajectories, solar sail, orbits for planetary observation and ascent trajectory of Launcher. He is an associate editor for the journals of Aerospace Science and Technology, and International Journal of Aerospace Engineering. E-mail: christian.circi@uniroma1.it.